

A Krylov-Subspace Technique for the Global Stability Analysis of Large Nonlinear Microwave Circuits

Vittorio Rizzoli (1), Franco Mastri (2), Elena Furini (1), and Alessandra Costanzo (1)

(1) DEIS, University of Bologna, Villa Griffone, 40044 Pontecchio Marconi (BO), Italy

(2) DIE, University of Bologna, Viale Risorgimento 2, 40136 Bologna, Italy

Abstract — The paper discusses a new approach to the global stability analysis of large nonlinear microwave circuits for which Nyquist's analysis is not usable owing to the size of the characteristic equation. Making use of a Krylov method for autonomous circuits, a state lying on the bifurcated branch close enough to the bifurcation may be efficiently located. The bifurcated branch may then be found by ordinary continuation.

I. INTRODUCTION

In recent years, the harmonic-balance (HB) technique coupled with Krylov-subspace methods has gained widespread acceptance as a numerical tool for the analysis of nonlinear microwave circuits containing large numbers of devices and/or supporting steady states with discrete spectra including large numbers of lines [1], [2]. However, the extension of these techniques to stability analysis has remained until now an unsolved problem. With harmonic balance, stability is normally investigated with the aid of Nyquist's analysis [3], [4]. A Nyquist plot may be numerically built by computing the determinant of the characteristic equation for a given steady state as a function of a perturbing frequency. After suitably parametrizing the circuit, the bifurcations may be located by searching for those combinations of frequency and parameter values for which the plot contains the origin of the complex plane [3], [4]. When the number of unknowns becomes very large, in order to waive the need for storing and factorizing the Jacobian matrix, HB analysis may be carried out by Krylov-subspace methods [1], [2]. Unfortunately, these methods do not provide an efficient way of computing the determinant of a large complex matrix, which prevents the use of Nyquist's analysis. In this paper we propose for the first time a family of algorithms based on Krylov-subspace HB whereby the fundamental bifurcations of a large-size circuit can be efficiently located. Hopf and period-doubling bifurcations are found by a Krylov-subspace technique specifically devised for autonomous nonlinear circuits. Regular turning points are detected by a suitable extension of a switching-parameter algorithm that was previously demonstrated in conjunction with ordinary HB.

II. BIFURCATION DETECTION FOR A LARGE CIRCUIT

Let the circuit be parametrized by some physical or electrical parameter u . On a given solution path, the bifurcating values of the parameter can be found with excellent approximation by the following approaches, relying upon Krylov-subspace HB as the basic analysis algorithm.

A. Hopf bifurcations of a DC solution path

In the state space, a periodic solution path bifurcates from the DC solution path at a Hopf bifurcation [5]. Let us consider a periodic steady state of fundamental frequency ω_F belonging to the bifurcated branch. Let \mathbf{E} be the vector of real and imaginary parts of the HB errors, and \mathbf{X} the state vector containing the real and imaginary parts of the state variable (SV) harmonics. \mathbf{E} and \mathbf{X} have a same dimension N . The HB solving system for such steady state may be cast in the form

$$\mathbf{E}(\mathbf{X}, \omega_F, u) = \mathbf{0} \quad (1)$$

The normal procedure to be followed in the construction of the periodic solution path would be to assign the free parameter u , and to solve then (1) for \mathbf{X} , ω_F . Note that the circuit is always autonomous with respect to the free oscillation, so that ω_F is always a problem unknown, and the phase ϕ_R of a reference harmonic X_R at frequency ω_F is indeterminate. ϕ_R is thus kept fixed to some arbitrary value, so that the correct number of unknowns is restored. Within the frame of ordinary HB techniques for autonomous circuits, the solution may be found by a Newton iteration after suitably modifying the state vector [6], or by resorting to continuation with artificial embedding [7] (usually, by introducing in the circuit suitable fictitious sources or "probes"). However, for reasons to be explained later on, in view of the application to large systems (say, $N \geq 25,000$) we do not want to modify the structure of the system (1) - specifically, of its Jacobian matrix. We do not want to use continuation, either, in order to minimize the number of CPU-intensive iterative solutions of (1). In order to overcome this problem, we retain the original formulation of the HB system, and remove the phase indeterminacy by adding to (1) an auxil-

iary equation whereby the phase of X_R is fixed to the selected value ϕ_R . This equation has the simple form

$$\sin(\phi_R) \operatorname{Re}[X_R] - \cos(\phi_R) \operatorname{Im}[X_R] = 0 \quad (2)$$

Let us now define $M_R = |X_R|$. When the circuit state approaches a Hopf bifurcation on the periodic solution path, then simultaneously $u \rightarrow u_B$, $\omega_F \rightarrow \omega_B$, $M_R \rightarrow 0$, where the subscript "B" denotes the bifurcating values. It is thus obvious that an approximate evaluation of u_B , ω_B , can be obtained by searching for a periodic regime having near-zero M_R . In other words, we can approximately locate the Hopf bifurcation by interchanging the roles of M_R and u , and treating the former as a known quantity to be fixed to some suitably small value, and the latter as a further problem unknown. Once again, this can be done by adding to (1), (2) a further auxiliary equation of the form

$$(\operatorname{Re}[X_R])^2 + (\operatorname{Im}[X_R])^2 - M_R^2 = 0 \quad (3)$$

In summary, the Hopf bifurcation can be approximately located by solving the nonlinear system of $N + 2$ equations in as many unknowns X , ω_F , u

$$\begin{cases} E(X, \omega_F, u) = 0 \\ \sin(\phi_R) \operatorname{Re}[X_R] - \cos(\phi_R) \operatorname{Im}[X_R] = 0 \\ (\operatorname{Re}[X_R])^2 + (\operatorname{Im}[X_R])^2 - M_R^2 = 0 \end{cases} \quad (4)$$

Note that M_R cannot be set to zero, since the Jacobian matrix would then become singular. Nevertheless, Hopf's theorem shows that $\partial u / \partial M_R = 0$ at criticality [5], which implies that the bifurcating parameter value u_B can be determined with excellent accuracy making use of relatively large values of M_R . The Jacobian matrix of (4) has the form

$$J = \left[\begin{array}{c|cc} J_{EX} & \frac{\partial E}{\partial \omega_F} & \frac{\partial E}{\partial u} \\ \hline R & 0 & 0 \end{array} \right] \quad (5)$$

In (5), $J_{EX} = \partial E / \partial X$ is the $N \times N$ Jacobian matrix of the standard HB system (1), $\partial E / \partial \omega_F$ and $\partial E / \partial u$ are column vectors of size N , and R is a $2 \times N$ matrix that can be readily obtained by inspection of (4). In the solution of (4) by iterative methods, most of the CPU time is spent in the multiplication of J times a sequence of real vectors [8]. In turn, due to (5), the dominant contribution to the cost of this process is given by the multiplication of J_{EX} , which can be accomplished by the efficient algorithms already demonstrated for the non-autonomous case [2]. The overhead due to the increased number of equations of (4) with respect to (1) is only $2N + 4$ flops (1 flop = 1 floating-point multiplication plus 1 addition), which is practically

negligible when N exceeds a few thousand. In this way a Hopf bifurcation may be efficiently located by a single inexact Newton iteration [2]. A similar algorithm can be used to detect the Hopf bifurcations of periodic solution paths. This technique is fast enough to allow the direct computation of Hopf bifurcations loci in a two-dimensional parameter space, which may often provide a useful support to the solution of design problems [9].

In order to accurately locate the bifurcation it is necessary that the analysis algorithm exhibits good convergence properties in a range of values of M_R where $\partial u / \partial M_R \approx 0$, which normally means, quite close to the bifurcation. When using a Krylov-subspace technique to solve the system (4), this may not be true for the GMRES iteration associated with an ordinary polynomial backtracking scheme [8] because the Jacobian matrix tends to be ill-conditioned in the neighborhood of the bifurcation. For this reason a novel trust-region algorithm [10] was implemented to increase the robustness of the Krylov-subspace solution method in the vicinity of a singularity of the Jacobian matrix. This algorithm is briefly discussed in section III.

B. Period-doubling bifurcations

A period-doubling (I-type) bifurcation of a periodic solution path [5] can be found by a similar algorithm. In this case $\omega_F = \omega_S/2$, where ω_S is the source frequency, so that the unknowns are X , u . Furthermore, the frequency division process is coherent, so that in this case there is no phase indeterminacy, and ϕ_R is a problem unknown. The nonlinear system used to locate the bifurcation thus becomes

$$\begin{cases} E(X, \frac{\omega_S}{2}, u) = 0 \\ (\operatorname{Re}[X_R])^2 + (\operatorname{Im}[X_R])^2 - M_R^2 = 0 \end{cases} \quad (6)$$

In turn, the Jacobian matrix is obtained from (5) by suppressing the second column (and the first row of R). The rest of the preceding discussion remains valid.

C. Regular turning points

In principle, regular turning points could be automatically detected during the construction of a solution path by ordinary continuation, since $\|Du/DX\| = 0$ at these points (D denotes the derivative taken along the solution path). However, at turning points the harmonic Jacobian is singular [5], so that these points cannot be approached by an analysis technique based on the Newton iteration. An efficient way of circumventing this problem is to perform a parameter switch near criticality, i.e., to replace u by a different parameter whose derivative does not vanish at the turning point [11]. A convenient choice is to use once

again the magnitude M_R of the reference harmonic. If the system is autonomous ω_F is unknown, so that the HB system to be solved in the neighborhood of the bifurcation is (4) with an arbitrary constant value of ϕ_R . If the circuit is forced, ω_F represents the forcing frequency (or the vector of independent forcing frequencies for a multitone regime) and is a priori known; the solving system is then obtained from (4) by suppressing the second equation. In both cases, u becomes a problem unknown and M_R plays the role of a known free parameter to be stepped across a suitable range containing the critical point. In order to detect the condition of approaching criticality, the quantity $\delta = \|Du/DX\|$ is monitored during the construction of the solution path. The parameter switching is automatically activated when δ drops below some empirically defined threshold, and is suppressed in the opposite condition.

III. A GLOBALLY CONVERGENT TRUST-REGION ALGORITHM

In order to improve the robustness of nonlinear solvers based on GMRES or similar iterative algorithms, a one-dimensional minimization of the error vector norm along the Newton update direction (backtracking) is usually carried out after each Newton step [8]. Nevertheless, for relatively ill-conditioned problems this approach may fail, and more robust search schemes must be implemented in support of the Newton iteration. A possible solution is to resort to the trust-region algorithm discussed in this section [10]. Let us rewrite the solving system (either (4) or (6) according to the previous discussion) in the unified form

$$F(U) = 0 \quad (7)$$

In a neighborhood of a generic iterate U , we may replace F by the linear model

$$F(U + d) \approx F(U) + J(U)d \quad (8)$$

where d is a sufficiently small increment. In turn, from (8) we obtain a local quadratic model of the scalar function to be minimized

$$\begin{aligned} f(U + d) &= \frac{1}{2} F^{\text{tr}}(U + d)F(U + d) \approx \\ &\approx \frac{1}{2} F^{\text{tr}}(U)F(U) + F^{\text{tr}}(U)J(U)d + \frac{1}{2} d^{\text{tr}}J^{\text{tr}}(U)J(U)d \end{aligned} \quad (9)$$

where tr denotes transposition. The spherical domain of radius τ where (9) represents a reliable approximation will be called a *trust region*. Let us denote by N the Newton update generated by the GMRES iteration. If $\|N - U\| \leq \tau$,

then $d = N - U$ minimizes (9) within the trust region. Otherwise the increment d that minimizes f within the trust is given by [10]

$$d(\mu) = -[J^{\text{tr}}(U)J(U) + \mu I]^{-1} J^{\text{tr}}(U)F(U) \quad (10)$$

where I is the identity matrix, for the unique $\mu \geq 0$ such that $\|d(\mu)\| = \tau$.

In practice, since μ cannot be computed exactly, $d(\mu)$ is approximated in the following way. We further introduce the *Cauchy point* C , defined as the point where (9) reaches a minimum along the steepest-descent direction $-\nabla F(U)$. We then consider the polygonal contour in the state space obtained by connecting the current update U to the Cauchy point C , and the latter to the Newton update N . Such contour is conventionally called the *dogleg curve* [10]. It can be shown that the point U_+ where the dogleg curve intersects the trust region boundary provides a good approximation to the minimum of f [10].

The trust region radius τ is updated until a reasonable agreement between $f(U_+)$ and its quadratic model (9) is achieved. The point U_+ generated in this way is chosen as the next iterate.

IV. AN EXAMPLE OF APPLICATION

Let us consider a typical single-conversion receiver front-end, consisting of two doubly-balanced mixers arranged in an image-rejection configuration, a local oscillator, coupling networks, amplifiers, and filters. The band of operation is 935 - 960 MHz with a fixed IF of 90 MHz. The nominal gate and drain bias voltages are $V_{GS} = -0.8$ V, $V_{DS} = 4.5$ V. The circuit-level description of the front-end is very detailed, and includes many (linear) parasitic components. The total number of device ports is $n_D = 208$, and the total number of nodes is 1744. The front-end is analyzed as a single circuit, so that inter-block couplings that may exist for various reasons such as imperfect isolation or proximity effects may be accounted for without difficulty. For illustrative purposes, a FET local oscillator is designed for 0 dBm output power at 857.5 MHz when biased at the nominal point and loaded by an ideal 50Ω resistance. After connecting the LO to the front-end, we want to determine the bifurcation pattern of the entire front-end parametrized by V_{DS} , starting from the Hopf bifurcation where the front-end turnon takes place. We consider standard operating conditions, with a -50 dBm RF signal at 947.5 MHz (corresponding to center band) received by the antenna. The circuit is strongly nonlinear and has a high gain, so that a relatively extended spectrum including intermodulation products of the RF and LO frequencies up to the 8th order is required in the HB analy-

sis. This results in 72 positive frequencies and 252,880 nodal unknowns. The reference harmonic is selected as the drain voltage harmonic of the oscillating transistor at the fundamental LO frequency, with $\phi_R = 0$. The Hopf bifurcation H is first located by solving (4) with $M_R = 0.1$ V and the remaining harmonics initialized to zero. The ordinary bctracking algorithm fails to converge in such situation; on the contrary, the GMRES/trust region iteration converges smoothly in about 1505 seconds on a SUN Enterprise 450 workstation, yielding $u_B \approx 1.2517$ V and $\omega_B/2\pi \approx 879.4$ MHz. Starting from the Hopf bifurcation, the front-end bifurcation diagram may be easily computed, and is shown in fig. 1 in terms of conversion gain versus drain voltage. The adopted value of M_R belongs to a parameter range where $\partial u / \partial M_R$ may be considered zero for all practical purposes. Indeed, the accuracy of the above quoted estimate of u_B turns out to be better than $4 \cdot 10^{-3}$. Fig. 2 shows the Hopf bifurcation locus in the two-dimensional parameter space (V_{GS} , V_{DS}). The front-end operation is impossible in the shaded area.

REFERENCES

- [1] M. M. Gourary et al., "Iterative solution of linear systems in harmonic balance analysis", *1997 IEEE MTT-S Int. Microwave Symp. Digest*, Denver, CO, June 1997, pp. 1507-1510.
- [2] V. Rizzoli et al., "Fast and robust inexact-Newton approach to the harmonic-balance analysis of nonlinear microwave circuits", *IEEE Microwave Guided Waves Lett.*, Vol. 7, Oct. 1997, pp. 359-361.
- [3] V. Rizzoli and A. Neri, "State of the art and present trends in nonlinear microwave CAD techniques", *IEEE Trans. Microwave Theory Tech.*, Vol. 36, Feb. 1988, pp. 343-365.
- [4] S. Basu, S. A. Maas, and T. Itoh, "Piecewise stability analysis in microwave circuits", *IEEE Microwave Guided Waves Lett.*, Vol. 5, May 1995, pp. 159-160.
- [5] J. Guckenheimer and P. Holmes, *Nonlinear Oscillations, Dynamical Systems, and Bifurcations of Vector Fields*. New York: Springer-Verlag, 1983.
- [6] V. Rizzoli and A. Neri, "Harmonic-balance analysis of multitone autonomous nonlinear microwave circuits", *1991 IEEE MTT-S Int. Microwave Symp. Digest*, Boston, MA, June 1991, pp. 107-110.
- [7] D. Hente and R. H. Jansen, "Frequency-domain continuation method for the analysis and stability investigation of nonlinear microwave circuits", *Proc. Inst. Elec. Eng., pt. H*, Vol. 133, Oct. 1986, pp. 351-362.
- [8] Y. Saad and M. H. Schultz, "GMRES: a generalized minimal residual method for solving nonsymmetric linear systems", *SIAM J. Sci. Stat. Comput.*, Vol. 7, July 1986, pp. 856-869.
- [9] V. Rizzoli and A. Neri, "The use of Hopf bifurcations loci for spurious-free nonlinear microwave circuit design", *1995 IEEE MTT-S Int. Microwave Symp. Digest* (Orlando), May 1995, pp. 1089-1092.
- [10] J. E. Dennis, R. B. Schnabel, *Numerical methods for unconstrained optimization and nonlinear equations*, Englewood Cliffs, NJ: Prentice-Hall, 1983.
- [11] V. Rizzoli, A. Costanzo, and A. Neri, "Automatic generation of the solution path of a parametrized nonlinear circuit in the presence of turning points", *Microwave Opt. Tech. Lett.*, Vol. 7, Apr. 20, 1994, pp. 270-274.

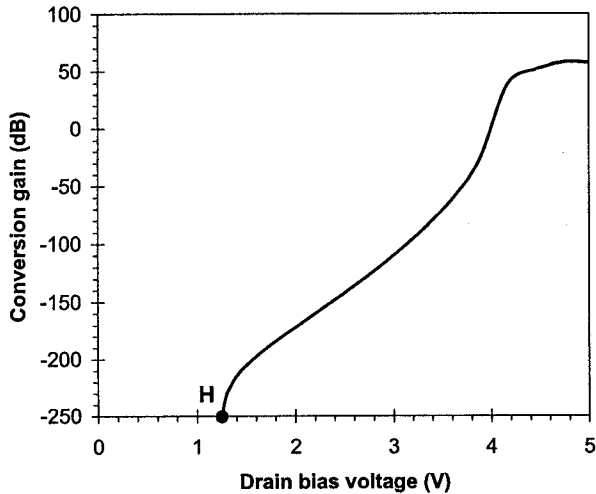


Fig. 1. Front-end bifurcation diagram.

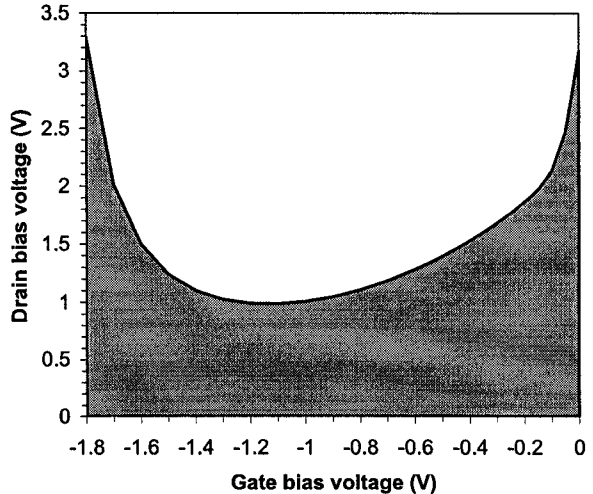


Fig. 2. Hopf bifurcation locus in the V_{GS} - V_{DS} plane.